

# Linköping University Postprint

## Energy distributions of positive and negative ions during magnetron sputtering of an Al target in Ar/O<sub>2</sub> mixtures

Jon M. Andersson, E. Wallin, E. P. Mürger & U. Helmersson

Original publication:

Jon M. Andersson, E. Wallin, E. P. Mürger & U. Helmersson, Energy distributions of positive and negative ions during magnetron sputtering of an Al target in Ar/O<sub>2</sub> mixtures, 2006, Journal of Applied Physics, (100), 033305.

<http://dx.doi.org/10.1063/1.2219163>.

Copyright: American Institute of Physics, <http://jap.aip.org/jap/top.jsp>

Postprint available free at:

Linköping University E-Press: <http://urn.kb.se/resolve?urn=urn:nbn:se:liu:diva-10472>

# Energy distributions of positive and negative ions during magnetron sputtering of an Al target in Ar/O<sub>2</sub> mixtures

Jon M. Andersson and E. Wallin

*IFM Material Physics, Linköping University, SE-581 83 Linköping, Sweden*

E. P. Münger

*IFM Theory and Modelling, Linköping University, SE-581 83 Linköping, Sweden*

U. Helmersson<sup>a)</sup>

*IFM Material Physics, Linköping University, SE-581 83 Linköping, Sweden*

(Received 15 March 2006; accepted 24 May 2006; published online 7 August 2006)

The ion flux obtained during reactive magnetron sputtering of an Al target in Ar/O<sub>2</sub> gas mixtures was studied by energy-resolved mass spectrometry, as a function of the total and O<sub>2</sub> partial pressures. The positive ions of film-forming species exhibited bimodal energy distributions, both for direct current and radio frequency discharges, with the higher energy ions most likely originating from sputtered neutrals. For the negative oxygen ions a high-energy peak was observed, corresponding to ions formed at the target surface and accelerated towards the substrate over the sheath potential. As the total pressure was increased the high-energy peaks diminished due to gas-phase scattering. Based on these results, the role of energetic bombardment for the phase constituent of alumina thin films are discussed. © 2006 American Institute of Physics.

[DOI: [10.1063/1.2219163](https://doi.org/10.1063/1.2219163)]

## I. INTRODUCTION

Alumina (Al<sub>2</sub>O<sub>3</sub>) thin films are used in a wide variety of applications, ranging from microelectronics to catalysts and wear-resistant coatings. Due to the existence of several metastable alumina phases, which frequently form in low-temperature growth situations (<1000 °C), precise control over crystalline phase formation is required during the film growth process in order to avoid undesired phases. In certain applications, e.g., catalysis, metastable phases are used, while in many other situations the thermally stable  $\alpha$  phase is desired. As a consequence, phase control of alumina thin films in general, and low-temperature growth of  $\alpha$ -Al<sub>2</sub>O<sub>3</sub> in particular, has been studied intensely during the last decade.<sup>1–6</sup>

Irradiation of the growth surface by energetic ions is known to be important in thin film growth, especially at low growth temperatures. For example, properties such as microstructure,<sup>7</sup> defect density,<sup>8</sup> and crystal structure<sup>9,10</sup> can effectively be modified by energetic bombardment. In two recent papers we have investigated low-temperature growth of  $\alpha$ -Al<sub>2</sub>O<sub>3</sub> thin films<sup>6</sup> as well as the contents of the deposition flux<sup>11</sup> during reactive radio frequency (rf) magnetron sputtering, with the aim to explain and achieve control over the growth process. In the present work, these studies are continued by measurements on the energies of the positive and negative ions in the deposition flux, as functions of total and O<sub>2</sub> partial pressures. Although deposition of alumina by reactive sputtering is a very active research field and of high industrial importance, the energy distributions of the depositing species have not been studied before. The results from

the measurements are used, together with our previous studies, to discuss the effects of energetic bombardment on alumina thin film growth.

## II. EXPERIMENTAL DETAILS

The experiments were performed in an ultrahigh vacuum (UHV) deposition system evacuated by a 450 l/s turbomolecular drag pump to a base pressure of  $<7 \times 10^{-7}$  Pa. The energy analysis probe consists of a differentially pumped energy-resolved mass spectrometer (Hiden Analytical Ltd. PSM 003), which was mounted with the sampling orifice ( $\varnothing$  300  $\mu$ m) facing the race track of the magnetron at a distance of 17 cm from the target surface. The front plate of the probe was electrically floating in all measurements. The Al target ( $\varnothing$  50 mm) was powered by either rf or direct current (dc) supplies in a mixed Ar+O<sub>2</sub> sputtering gas. Unless otherwise stated the supplies were run at constant powers of 80 and 50 W, respectively. The O<sub>2</sub> partial pressure was measured during sputtering by the mass spectrometer and separately calibrated using a system pressure gauge.

The ion beam focusing voltages of the mass spectrometer were carefully tuned to optimize sensitivity for ions of all energies of interest (i.e., not only the energy of the plasma potential peak, which is the default setting), in order to give a more realistic description of the ion flux. Still, it should be stressed that these measurements are qualitative and subject to some uncertainties regarding, e.g., the relative heights of low- and high-energy peaks. In the presented energy distributions the high-frequency noise has been removed by fast Fourier transform filtering.

<sup>a)</sup>Electronic mail: [ulfhe@ifm.liu.se](mailto:ulfhe@ifm.liu.se)

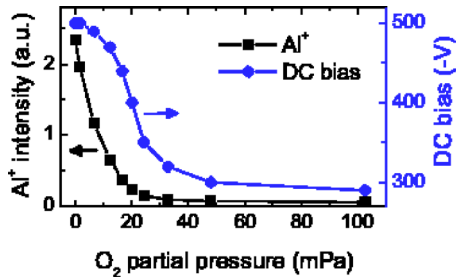


FIG. 1. (Color online) Measured  $\text{Al}^+$  intensity compared to the target self-bias voltage as functions of  $\text{O}_2$  partial pressure. Also reported in Ref. 11.

### III. RESULTS AND DISCUSSION

The presentation of our results is divided into four main parts. First, the target oxidation process is described for our particular setup. Then, the energy-resolved measurements on positive (rf and dc sputtering) and negative ions (rf) are presented, and finally, the effects of bombardment on alumina thin film growth are discussed in view of the results from Refs. 6 and 11

#### A. The target oxidation process

This section contains results already presented in Ref. 11 which are needed as a background to define the experimental conditions of the measurements presented in the subsequent sections.

During reactive sputtering of Al in an Ar+ $\text{O}_2$  mixture, the transition between metallic and oxidized target modes is typically very abrupt.<sup>12</sup> This is due to the high oxygen affinity of Al, making the target and deposited metal a very effective getter pump. As the metal is fully oxidized this “extra pump” vanishes and the consumption of oxygen drops, which for many sputtering setups results in a strong hysteresis in the  $\text{O}_2$  partial pressure, target voltage, and deposition rate.<sup>13</sup> In the present case, however, the small target area and high pumping speed lessened the effect of the extra pump and, hence, removed the problematic hysteresis behavior.<sup>13</sup> Thus, the measured  $\text{Al}^+$  intensity and target (self-bias) voltage,<sup>11</sup> shown in Fig. 1, displayed no hysteresis effects.

The expected drops in  $\text{Al}^+$  signal and target voltage, as the target shifts from metallic to oxidized mode, are clearly seen in Fig. 1. An interesting observation, previously mentioned by Maniv and Westwood,<sup>12</sup> is the decrease in  $\text{Al}^+$  intensity (and deposition rate<sup>6</sup>) with increasing  $\text{O}_2$  partial

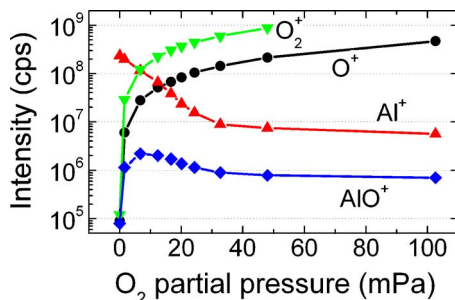


FIG. 2. (Color online) Measured intensities of the main film-forming ions as functions of  $\text{O}_2$  partial pressure at a total pressure of 0.33 Pa. Also reported in Ref. 11.

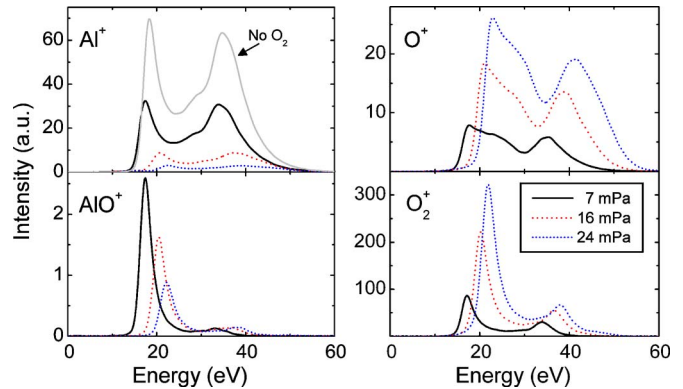


FIG. 3. (Color online) Energy distributions of the main film-forming ions, during rf magnetron sputtering, for three different  $\text{O}_2$  partial pressures at a total pressure of 0.33 Pa. For  $\text{Al}^+$  also the distribution recorded in a pure Ar discharge is shown.

pressure, which occurred before the target voltage had started to change. The unaffected voltage indicates that the target was still in the metallic mode, while the reduction in  $\text{Al}^+$  is most likely due to oxygen reactions at the target surface, occurring prior to the formation of an oxide compound. The occurrence of such reactions is strongly supported by our recent report on AlO molecules,<sup>11</sup> sputtered from the target.

Figure 2 shows the measured (integrated) ionic intensities of the main film-forming ions ( $\text{O}^+$ ,  $\text{O}_2^+$ ,  $\text{Al}^+$ , and  $\text{AlO}^+$ ) in the sputtering plasma, as functions of  $\text{O}_2$  partial pressure, showing, e.g., up to about 10%  $\text{AlO}^+$  relative to  $\text{Al}^+$ . As shown in Ref. 11 the amounts of neutral AlO (compared to Al) are considerably higher due to differences in ionization probabilities.

#### B. Positive ions

In this section the energy distributions of the positive ions are first presented and then the origin of the high-energy ions and the effect of the  $\text{O}_2$  partial pressure are discussed. The influence of the ions on thin film growth is treated in Sec. III D.

##### 1. rf sputtering

Figure 3 shows the measured energy distributions of the main film-forming ions incident onto the substrate during rf sputtering at different  $\text{O}_2$  partial pressures and a total pressure of 0.33 Pa. In all cases the distributions are bimodal with two broad peaks, the second (high-energy) peak being

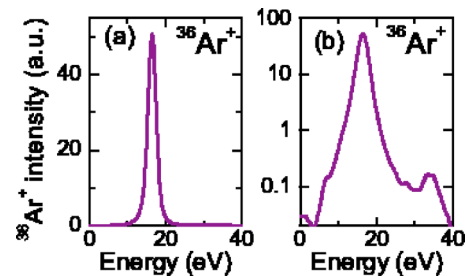


FIG. 4. (Color online) Typical energy distribution for  $^{36}\text{Ar}^+$  in (a) linear and (b) logarithmic scales during rf sputtering at 0.33 Pa total pressure.

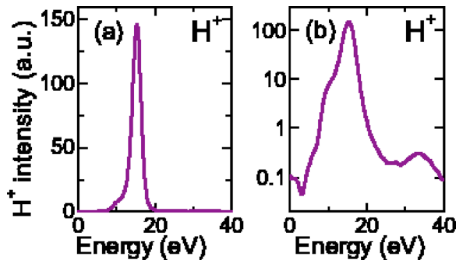


FIG. 5. (Color online) Typical energy distributions for  $H^+$  in (a) linear and (b) logarithmic scales, as measured during rf sputtering at 0.33 Pa total pressure.

less pronounced for the molecular ions. Although the total fluxes of the ions vary with  $O_2$  pressure (see also Fig. 2), there are no clear changes in the shapes of the distributions. Figures 4 and 5 show typical distributions for  $^{36}Ar^+$  and  $H^+$  ions. No significant changes were observed for different  $O_2$  partial pressures, except shifts due to changes in the plasma potential. In linear scale the  $^{36}Ar^+$  and  $H^+$  distributions appear to be single peaked, whereas the logarithmic graphs reveal small high-energy peaks also for these ions. Figure 6 shows typical  $Al^+$  and  $O^+$  energy distributions at a total pressure of 0.67 Pa. At this higher pressure the high-energy peaks are significantly smaller relative to the first peak. The origin of the bimodal distributions is further discussed in Sec. III B 3.

## 2. dc sputtering

To clarify the interpretation of the measurements made during rf sputtering, comparable measurements were made also for a dc magnetron discharge. Figure 7 shows typical resulting energy distributions for  $Al^+$  and  $O^+$  at a total pressure of 0.33 Pa. The sharp low-energy peak corresponds to thermalized ions, which have been accelerated from the plasma potential to the probe, while the broad distribution at higher energies is interpreted as originating from sputtered neutrals which have been postionized, by electron impact, in the plasma and then reached the probe without collisions. The general appearance of the second peak is similar to typical measured energy distributions of sputtered neutrals,<sup>14–17</sup> and to distributions resulting from the Thompson random collision cascade model.<sup>18</sup> However, although the measured ion energy distributions are expected to reflect the distributions of the sputtered neutrals, the kinetic energies of the ions can be subject to a small shift, since the plasma potential might not be perfectly constant within the plasma.<sup>19</sup>

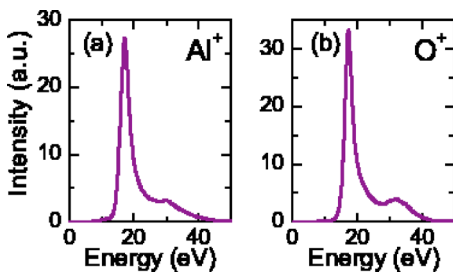


FIG. 6. (Color online) Typical energy distributions of (a)  $Al^+$  and (b)  $O^+$  in a rf sputtering plasma at a total pressure of 0.67 Pa.

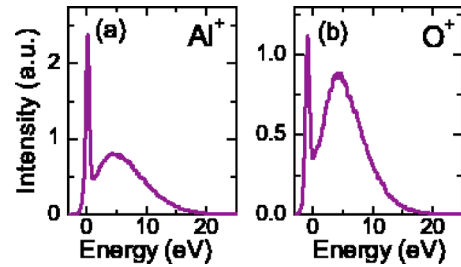


FIG. 7. (Color online) Typical energy distributions for (a)  $Al^+$  and (b)  $O^+$  recorded in a dc magnetron discharge at a total pressure of 0.33 Pa.

## 3. Origin of the high-energy ions in the rf discharge

It seems evident that the postionized sputtered neutrals, which were observed in the dc discharge, should be present also during rf magnetron sputtering. However, since the ion energy distributions are very different with more complex shapes and higher ion energies in the rf case, some further experiments were performed in order to elucidate the origin of the energetic ions. In Sec. III B 1 it was shown that large high-energy peaks were seen only for species originating from the target and not for Ar or H, and also that the second peak diminishes as the total pressure increases. The same was seen as a shutter blocked the direct path between target and probe (Fig. 8) and as the magnetron was placed facing the mass spectrometer at an angle of  $45^\circ$  (not shown). Thus, we conclude that the high-energy peaks in the distributions of Fig. 3 do indeed originate from neutrals sputtered from the target. The same conclusions were drawn, based on similar arguments, by other authors who have also measured high-energy peaks in magnetron sputtering discharges.<sup>20–22</sup>

It should be mentioned that bimodal ion energy distributions frequently appear in rf sputtering plasmas due to rf modulations.<sup>23,24</sup> Such effects produce a clear mass dependence in the peak separation, i.e., lighter (more mobile) ions show a larger separation.<sup>23</sup> This was not observed in the present case. Hence, as shown also in the previous paragraph, rf effects are not the reason for the existence of high-

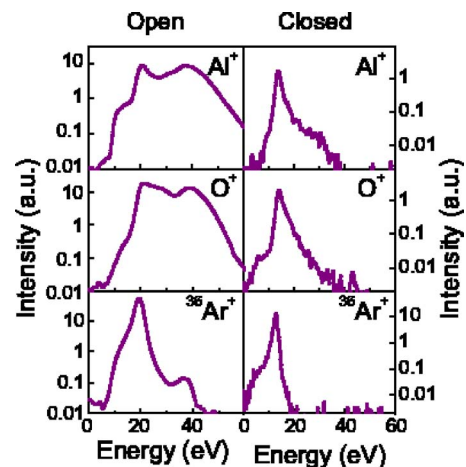


FIG. 8. (Color online) Comparison of energy distributions for  $Al^+$ ,  $O^+$ , and  $^{36}Ar^+$ , during rf sputtering at 0.33 Pa, with or without a shutter blocking the path between the target and the mass spectrometer.

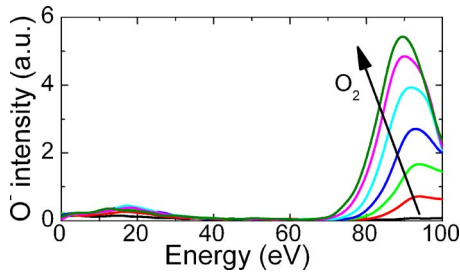


FIG. 9. (Color online) Energy distributions of  $O^-$  for seven  $O_2$  partial pressures ranging from 13 to 227  $\mu\text{Pa}$ , with the arrow indicating increasing  $O_2$  pressure. The total pressure was 0.33 Pa.

energy peaks. Still, we have to assume that the more complex and broader shapes of the distributions, compared to the dc case, are caused by the rf field.

### C. Negative ions

During sputtering of oxide or oxidized metal targets, significant amounts of negative oxygen ions can form at the target surface and be accelerated to high energies over the target sheath potential.<sup>25,26</sup> If these energetic particles bombard the substrate, they can strongly influence the growing film.<sup>27</sup> To determine their importance on alumina thin film growth the energy distributions of  $O^-$  ions were recorded during reactive rf magnetron sputtering of Al.

The target sheath voltage in the thin film growth process<sup>6</sup> is about  $-500$  to  $-300$  V, as inferred from Fig. 1. Since the mass spectrometer used here is limited to ion energies below 100 eV, the rf power was reduced to enable detection of energetic  $O^-$ . As a consequence, both the sputter rate and the  $O_2$  partial pressures are lower compared to those used for the measurements on the positive ions.

Figure 9 shows recorded  $O^-$  energy distributions for different  $O_2$  partial pressures at a total pressure of 0.33 Pa. There are distinct peaks in the distributions corresponding to  $O^-$  ions that have been accelerated over the target sheath voltage and reached the probe without collisions. In Fig. 10, the height of these peaks is compared to the target voltage, as a function of the  $O_2$  partial pressure. The amount of energetic oxygen increases strongly in the transition region between the metallic and oxidized modes of the target and then levels out as the target becomes oxidized. Figure 11 displays the dependence of the  $O^-$  energy distributions on total sputtering pressure in the fully oxidized target mode. As the total pressure increases from 0.33 to 0.67 Pa, which are the pressures

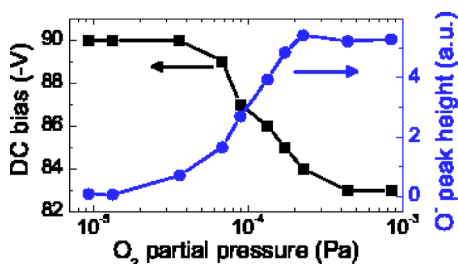


FIG. 10. (Color online) Target self-bias voltage compared to peak heights of the  $O^-$  high-energy peaks as functions of  $O_2$  partial pressure. The total pressure was 0.33 Pa.

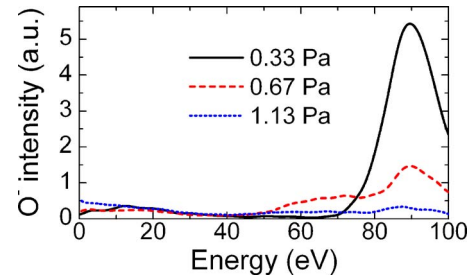


FIG. 11. (Color online)  $O^-$  energy distributions for different total pressures and a target self-bias voltage of about  $-80$  V. The target was operated in the fully oxidized mode.

used in the growth study in Ref. 6, the amount of high-energy oxygen is seen to decrease dramatically due to gas-phase collisions.

### D. Effects of bombardment on thin film growth

In the thin film growth study<sup>6</sup> it was shown that the  $\alpha$  phase formed at relatively high  $O_2$  partial pressure in combination with a low total pressure (0.33 Pa), while  $\gamma\text{-Al}_2\text{O}_3$  formed at a higher total pressure (0.67 Pa). All films were grown onto chromia nucleation layers at a relatively low growth temperature of  $500^\circ\text{C}$ . The dependence on total pressure suggests that  $\alpha\text{-Al}_2\text{O}_3$  formation was promoted by energetic bombardment, while the need for relatively high oxygen pressures demonstrates the important role of oxygen in the growth process used.

Previous works, on ionized physical vapor deposition, have shown that the crystal structure of alumina films is strongly influenced by energetic bombardment during growth.<sup>10,28,29</sup> Importantly, in relation to the present work, the  $\alpha$  phase was promoted in those studies by high energies ( $>100$  eV) of the depositing species, achieved by the applied substrate bias. In our case<sup>6</sup> no bias was applied and, as judged from the dc measurements presented in Fig. 7, the energies of the sputtered neutrals depositing onto the growth surface are distributed around a few eV with a tail extending to higher energies. In view of the previous studies, the energies of these particles should be too low to induce the observed changes in crystalline phase.

A possible source of high-energy particles is Ar neutrals backscattered from the target. We performed SRIM (Ref. 30) calculations on 0.5 keV Ar bombardment in order to estimate the significance of these particles. The calculations show that less than 0.1% and 0.01% of the incident Ar ions are backscattered from Al and  $\text{Al}_2\text{O}_3$  targets, respectively, due to the relatively low mass of the target atoms. These values can be compared to sputter yields of 0.69 and 0.32 for Al atoms sputtered from Al and  $\text{Al}_2\text{O}_3$  targets, respectively, as attained from the same calculations. We conclude that backscattered Ar does not play an important role in the presently studied growth process.

The energetic oxygen negative ions/atoms (see Sec. III C) bombarding the substrate have high kinetic energies, since they are accelerated over the target sheath voltage (300–500 eV in Ref. 6). Based on the conclusions of the above mentioned works,<sup>10,28,29</sup> such energetic particles can

induce the observed phase changes. Moreover, as shown in Sec. III C, the amount of energetic oxygen increases strongly as the target is oxidized and diminishes as the total pressure is increased from 0.33 to 0.67 Pa. This is consistent with the growth results, i.e., there is a clear correlation between  $\alpha$ -alumina formation and the presence of energetic oxygen. This suggests that bombardment by energetic oxygen ions/atoms was responsible for the observed changes from  $\gamma$ - to  $\alpha$ -alumina formation.<sup>6</sup> This conclusion is based on the assumption that the amount of energetic oxygen is high enough, relative to the total deposition flux. This assumption is difficult to verify by the measurements made here, but a comparison can be made with the study of Kester and Messier.<sup>27</sup> They studied the effects of energetic oxygen during sputtering of other oxides in terms of resputtering of the films and changes in microstructure indicative of energetic bombardment. Although they did not study the Al/O system, it can be inferred from their work that the amount of O<sup>-</sup> produced should be high enough to cause significant bombardment effects.

#### IV. CONCLUSION

We have studied the energy distributions of the ionic deposition flux during reactive magnetron sputtering of an Al target in Ar/O<sub>2</sub> gas mixtures. The aim of the study was to correlate the measured ion energies to previous alumina thin film growth results,<sup>6</sup> which showed changes in crystalline phase, plausibly induced by energetic bombardment.

The measurements presented here showed that each of the positive film-forming ions (O<sup>+</sup>, O<sub>2</sub><sup>+</sup>, Al<sup>+</sup>, and AlO<sup>+</sup>) exhibited a bimodal energy distribution with a large high-energy peak (in addition to the low-energy peak corresponding to thermalized ions), both for rf and dc sputtering discharges. We interpret the higher energy species as originating from the cathode. Bombardment by these species will increase the mobility at the growth surface, but, according to previous works,<sup>10,28,29</sup> should not be energetic enough to induce the observed phase changes. In contrast, the measurements show that the more energetic negative oxygen ions are a likely explanation for the observed film results. In the transition region between metallic and oxidized modes of the target—where the phase changes in grown films were observed<sup>6</sup>—the amount of energetic negative oxygen ions increased strongly. Moreover, as the total pressure was increased from 0.33 to 0.67 Pa the high-energy peak decreased dramatically due to gas-phase collisions, also in agreement with the film growth results. Thus, energetic bombardment, in the present case by negative oxygen ions, is identified (in

conjunction with nucleation control<sup>4</sup>) as a means of controlling crystalline phase formation during low-temperature growth of alumina thin films.

#### ACKNOWLEDGMENTS

The authors would like to thank J. Böhlmark, Y. Gonzalvo, and J. T. Gudmundsson for discussions concerning the mass spectrometer measurements. The Swedish Research Council (VR) is acknowledged for financial support.

- <sup>1</sup>O. Zywitzki, G. Hoetzsch, F. Fietzke, and K. Goedicke, *Surf. Coat. Technol.* **82**, 169 (1996).
- <sup>2</sup>J. M. Schneider, W. D. Sproul, A. A. Voevodin, and A. Matthews, *J. Vac. Sci. Technol. A* **15**, 1084 (1997).
- <sup>3</sup>P. Jin, G. Xu, M. Tazawa, K. Yoshimura, D. Music, J. Alami, and U. Helmersson, *J. Vac. Sci. Technol. A* **20**, 2134 (2002).
- <sup>4</sup>J. M. Andersson, Zs. Czígány, P. Jin, and U. Helmersson, *J. Vac. Sci. Technol. A* **22**, 117 (2004).
- <sup>5</sup>O. Kyrilov, D. Kurapov, and J. M. Schneider, *Appl. Phys. A: Mater. Sci. Process.* **80**, 1657 (2004).
- <sup>6</sup>J. M. Andersson, E. Wallin, U. Helmersson, U. Kreissig, and E. P. Münger, *Thin Solid Films* **513**, 57 (2006).
- <sup>7</sup>I. Petrov, L. Hultman, U. Helmersson, J.-E. Sundgren, and J. E. Greene, *Thin Solid Films* **169**, 299 (1989).
- <sup>8</sup>L. Hultman, S. A. Barnett, J.-E. Sundgren, and J. E. Greene, *J. Cryst. Growth* **92**, 639 (1988).
- <sup>9</sup>J. E. Greene and S. A. Barnett, *J. Vac. Sci. Technol.* **21**, 285 (1982).
- <sup>10</sup>J. Rosén, S. Mráz, U. Kreissig, D. Music, and J. M. Schneider, *Plasma Chem. Plasma Process.* **25**, 303 (2005).
- <sup>11</sup>J. M. Andersson, E. Wallin, E. P. Münger, and U. Helmersson, *Appl. Phys. Lett.* **88**, 054101 (2006).
- <sup>12</sup>S. Maniv and W. D. Westwood, *J. Appl. Phys.* **51**, 718 (1980).
- <sup>13</sup>See, e.g., S. Berg and T. Nyberg, *Thin Solid Films* **476**, 215 (2005).
- <sup>14</sup>R. V. Stuart and G. K. Wehner, *J. Appl. Phys.* **35**, 1819 (1964).
- <sup>15</sup>R. V. Stuart, G. K. Wehner, and G. S. Anderson, *J. Appl. Phys.* **40**, 803 (1969).
- <sup>16</sup>A. Cortona, W. Husinsky, and G. Betz, *Phys. Rev. B* **59**, 15495 (1999).
- <sup>17</sup>M. L. Yu, D. Grischkowsky, and A. C. Balant, *Phys. Rev. Lett.* **48**, 427 (1982).
- <sup>18</sup>M. W. Thompson, *Philos. Mag.* **18**, 377 (1968).
- <sup>19</sup>See, e.g., D. J. Field, S. K. Dew, and R. E. Burrell, *J. Vac. Sci. Technol. A* **20**, 2032 (2002).
- <sup>20</sup>K. Ellmer and D. Lichtenberger, *Surf. Coat. Technol.* **74–75**, 586 (1995).
- <sup>21</sup>H. Kersten, G. M. W. Kroesen, and R. Hippler, *Thin Solid Films* **332**, 282 (1998).
- <sup>22</sup>R. Roth, J. Schubert, and E. Fromm, *Surf. Coat. Technol.* **74–75**, 461 (1995).
- <sup>23</sup>J. W. Coburn and E. Kay, *J. Appl. Phys.* **43**, 4965 (1972).
- <sup>24</sup>E. Kawamura, V. Vahedi, M. A. Lieberman, and C. K. Birdsall, *Plasma Sources Sci. Technol.* **8**, R45 (1999).
- <sup>25</sup>K. Tominaga, T. Murayama, Y. Sato, and I. Mori, *Thin Solid Films* **343–344**, 81 (1991).
- <sup>26</sup>K. Tominaga, S. Iwamura, Y. Shintani, and O. Tada, *Jpn. J. Appl. Phys., Part 1* **21**, 688 (1982).
- <sup>27</sup>D. J. Kester and R. Messier, *J. Vac. Sci. Technol. A* **4**, 496 (1986).
- <sup>28</sup>Q. Li, Y.-H. Yu, C. Singh Bhatia, L. D. Marks, S. C. Lee, and Y. W. Chung, *J. Vac. Sci. Technol. A* **18**, 2333 (2000).
- <sup>29</sup>R. Brill, F. Koch, J. Mazurelle, D. Levchuk, M. Balden, Y. Yamada-Takamura, H. Maier, and H. Bolt, *Surf. Coat. Technol.* **174–175**, 606 (2003).
- <sup>30</sup>J. F. Ziegler and J. P. Biersack, [www.srim.org](http://www.srim.org)